Vortex Lattice Symmetry and Electronic Structure in $YBa_2Cu_3O_7$

B. Keimer,[1,2,3] W. Y. Shih,[2] R. W. Erwin,[3] J. W. Lynn,[3] F. Dogan,[2,4] and I. A. Aksay[2,4]

[1]*Department of Physics, Princeton University, Princeton, New Jersey 08544*

[2]*Princeton Materials Institute, Princeton University, Princeton, New Jersey 08544*

[3]*National Institute of Standards and Technology, Gaithersburg, Maryland 20899*

[4]*Department of Chemical Engineering, Princeton University, Princeton, New Jersey 08544*

(Received 31 May 1994)

We report a small angle neutron scattering study of the vortex lattice in $YBa_2Cu_3O_7$ in magnetic fields of $0.5 \leq H \leq 5$ T applied along and close to the c axis. Over the entire field range, the vortices form an oblique lattice with two nearly equal lattice constants and an angle of 73° between primitive vectors. Numerical calculations suggest that variations of the superconducting order parameter near the vortex core are important in stabilizing this structure. An analysis that accounts for the fourfold symmetry of the vortex core qualitatively explains both the symmetry and the orientation of the observed vortex lattice. A quantitative explanation of our data will require calculations based on a realistic gap equation.

PACS numbers: 74.60.Ec, 74.25.Ha

The cuprate high temperature superconductors have attracted a high level of interest both because of their unusual microscopic electronic structure and because of the novel properties and phases of the vortex system. We present small angle neutron scattering (SANS) data, as well as numerical calculations which suggest an intimate relation between the equilibrium structure of the vortex lattice in laboratory magnetic fields and the microscopic electronic structure of $YBa_2Cu_3O_7$.

In general, the free energy of a given vortex lattice structure depends on the magnetic field and materials parameters such as the penetration depth λ and coherence length ξ. Near the upper critical field H_{c2} the magnetic induction is almost uniform, and the vortex lattice free energy is determined exclusively by energies associated with perturbations of the superconducting order parameter. For isotropic superconductors, it has been shown [1] that, independent of λ and ξ, the lowest free energy belongs to the triangular lattice. It is also known [2–4] that for superconductors with anisotropic band structures and/or energy gaps, vortex lattice structures different from the triangular lattice can occur near H_{c2}, depending on the direction of the applied magnetic field with respect to the crystal lattice. These structures generally have a fixed orientation with respect to the crystalline axes.

Near the lower critical field H_{c1} the vortex lattice structure depends on the ratio $\kappa = \lambda/\xi$. For low-κ type-II superconductors such as Nb ($\kappa \sim 1$), ξ is comparable to intervortex distances even near H_{c1}. Because of spatial variations of the order parameter, the intervortex interaction acquires an attractive part in addition to the usual electrodynamic repulsion. The anisotropy of the electronic structure remains relevant near H_{c1}, and a variety of vortex lattice structures ranging from triangular to square has been observed [5,6]. By contrast, in extreme type-II superconductors such as $YBa_2Cu_3O_7$ ($\kappa \sim 100$) or $NbSe_2$ ($\kappa \sim 25$), ξ is negligible compared to the intervortex distance near H_{c1}, the vortices interact purely electrodynamically, and the vortex lattice structure is expected to be triangular with no preferred orientation with respect to the crystalline axes. These expectations have been confirmed by Bitter decoration experiments in very small magnetic fields [7,8]. Experiments in higher fields have thus far focused on the effects of the uniaxial anisotropy due to the layered structure of these materials [9–12]. The observed orientation of the vortex lattice in fields inclined with respect to the c axis disagrees with the one predicted by a purely electrodynamic model ("London theory") [13] for both $YBa_2Cu_3O_7$ [10,11] and $NbSe_2$ [12]. Based on our new experimental and numerical data, we argue here that even in laboratory fields far below H_{c2}, the spatial variation of the order parameter near the vortex core is important in determining both the symmetry and the orientation of the vortex lattice, thus explaining the disagreement with London theory.

The SANS experiments were carried out at the Cold Neutron Research Facility at NIST on the NG-3 and NG-7 spectrometers. $A \sim 2.5$ cm^3 $YBa_2Cu_3O_7$ single crystal, the same as we used in previous SANS experiments [10], was mounted in a horizontal-field superconducting magnet. The experiments were performed in the standard geometry with the magnetic field almost parallel to the neutron beam. Typical diffraction patterns for field orientations along and near the crystalline c axis are shown in Fig. 1.

We used neutrons of wavelength 5 or 6 Å and $\Delta\lambda/\lambda = 0.31$, source and sample apertures of 5 and 1.27 cm diameter, respectively, and source-to-sample distances between 11 and 13 m. The sample-to-detector distance was 15.9 m at $H = 0.5$ T, 10.6 m at $H = 2$ T, and 6.6 m at $H = 5$ T. While the longitudinal momentum resolution $\Delta q_{\parallel}$ becomes markedly wider as the sample-to-detector distance is reduced, the transverse momentum resolution $\Delta q_{\perp}$ is relatively insensitive to changes in this parameter [14]. This effect is responsible for the

0031-9007/94/73(25)/3459(4)$06.00

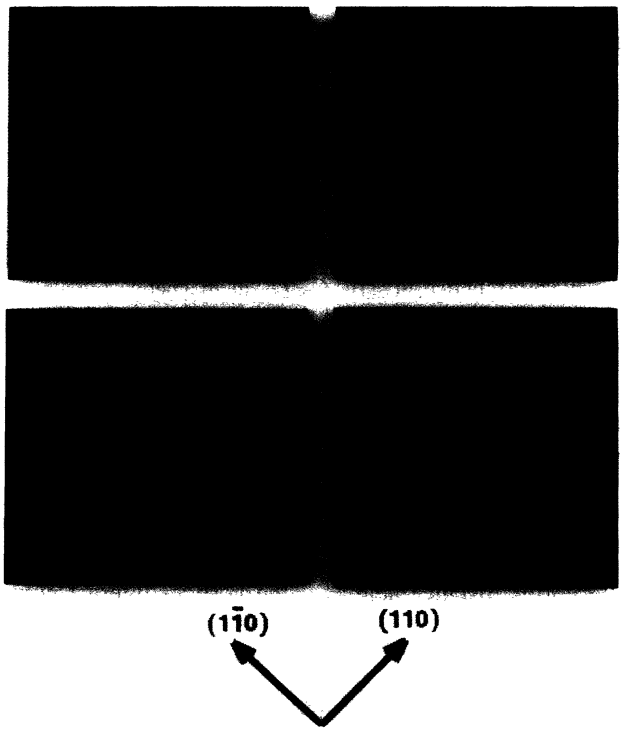

FIG. 1. SANS diffraction patterns of the vortex lattice taken for $H = 0.5$ T (top left), $H = 2$ T (top right and bottom left), and $H = 4.3$ T (bottom right), under experimental conditions described in the text. The temperature is 4.2 K, and the magnetic field is perpendicular to the page. Patterns in the bottom row are taken with the magnetic field parallel to the c axis, while for the patterns in the top row the c axis subtends angles of $\sim 10°$ (left) [10] or 20° (right) with the field. The (110) and (1$\bar{1}$0) directions of the crystal lattice are indicated. The Bragg angles corresponding to the diffraction spot positions depend on the experimental conditions, so that they cannot be directly inferred from the patterns shown or compared between panels. For clarity the data were digitally smoothed on a scale comparable to the geometrical resolution.

ellipsoidal diffraction spots in Fig. 1, all of which are resolution limited. The resolutions $\Delta\varphi = \Delta q_\perp/q$ in the azimuthal angle φ perpendicular to the magnetic field are $\Delta\varphi = 24.5°$ (full width at half maximum) for $H = 0.5$ T, $\Delta\varphi = 10.4°$ for $H = 2$ T, and $\Delta\varphi = 6.1°$ for $H = 5$ T. The angular resolution of our diffraction patterns is therefore improved by up to a factor of 4 over previous measurements [10,11].

The advantage of the improved angular resolution becomes apparent on inspection of the $H = 2$ T diffraction pattern in the bottom left panel of Fig. 1: A total of 16 weak and 4 strong diffraction spots can be resolved. (Since only a subset of these 20 spots satisfies the Bragg condition simultaneously within the given resolution, not all of the spots appear in a single diffraction pattern such as the one shown in the figure.) In correlating this diffraction pattern with a real-space structure we first note that only Bravais lattices of singly quantized vortices need to be considered; because of flux quantization, non-Bravais lattices or lattices comprised of doubly quantized vortices would have larger unit cells inconsistent with our data. A superposition of four real-space domains as depicted in Fig. 2 provides a quantitative explanation for the observed pattern. (The diffraction pattern of a two-dimensional Bravais lattice can be obtained from the real lattice by a 90° rotation and rescaling.) While the strong diffraction spots are common to two of these four domains, the weak spots belong to just one domain and are therefore approximately half as bright as the strong spots. One of the principal axes of the vortex lattice coincides with either the (110) or the (1$\bar{1}$0) direction of the crystal lattice; the direction of the other axis is not obviously related to a crystalline high symmetry direction. An accurate measurement of the lattice parameters with high longitudinal resolution ($\Delta\lambda/\lambda = 0.14$) yielded the lattice constants 332 ± 15Å [along (110)] and 344 ± 15Å and an angle $\beta = 73° \pm 1°$ between primitive vectors for $H = 2$ T. Since the small systematic difference between the lattice constants is within the experimental resolution, our data are consistent with either oblique or centered rectangular vortex lattice symmetry. The same real-space structure also explains diffraction patterns taken for $H = 0.5$, 4.3, and 5 T (not shown). However, two of the weak spots remain unresolved with the spectrometer settings that had to be chosen at $H = 0.5$ T.

In this picture the fourfold symmetry of the diffraction patterns in the bottom row of Fig. 1 ($\mathbf{H} \parallel \mathbf{c}$) arises from the orientational alignment of the vortex lattice and the crystal lattice, which is fourfold symmetric in this direction. All four domains of Fig. 2 must therefore be equally populated in macroscopic regions of the sample. When the field is tilted with respect to the c axis, this argument no longer holds. We indeed observe diffraction patterns of lower symmetry in slightly inclined fields (top panels in Fig. 1), where the degeneracy of the four domains is broken and only two of the domains are populated. Possible physical origins of this domain imbalance are pinning interactions between vortices and twin boundaries [10], the uniaxial anisotropy [13], or a combination of these effects. For larger tilt angles, we observe a sequence of structural transitions and reorientations in [10,15].

Since in the cuprate superconductors H_{c2} is extremely large, the London model, believed to be valid for $\kappa \gg 1$ and $H \ll H_{c2}$, has been the basis for discussions of the equilibrium vortex lattice structure in these materials. Previously [16,17] the free energies of the triangular and the square lattice have been compared for isotropic superconductors in this limit, but the free energies of oblique structures such as the one we observe experimentally have thus far not been computed. We therefore decided to numerically evaluate the free energy of such vortex lattices as a function of the angle β between the primitive vectors. For simplicity we chose the centered rectangular structure (two equal lattice constants). $\beta = 60°$ thus corresponds to the triangular lattice, $\beta = 90°$ to the square lattice.

In the London approximation, the Gibbs free energy density of a given vortex lattice at the applied field H can

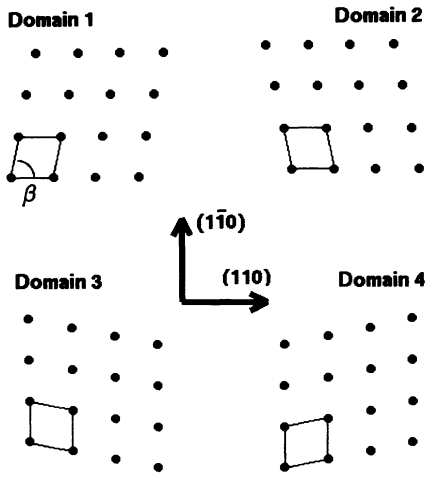

FIG. 2. The four real-space orientational domains of the vortex lattice formed for magnetic fields applied parallel or nearly parallel to the c axis. An appropriate superposition of the diffraction patterns from these domains explains the data of Fig. 1. The top row of that figure is taken under conditions in which only two of the domains are populated (1 and 2 or 3 and 4). In the bottom row all four domains are populated.

be written as [18]

$$G = \frac{B^2}{8\pi}\left(\sum_Q \frac{1}{1+\lambda^2 Q^2}\right) - \frac{HB}{4\pi}, \qquad (1)$$

where the sum runs over all reciprocal lattice vectors Q and is cut off at a circular "hard core" $Q_{\max} = 2\pi/\xi$. The magnetic induction B is computed for each lattice by setting $\partial G/\partial B = 0$. Since the lattice constant of the vortex lattice depends on B through the flux quantization rule, this equation is highly nonlinear. However, the fact that at a given applied field the magnetic induction B is different for each β is important, and our conclusions would be quite different if we compared different lattices at the same B [16,17]. The results of the numerical calculations with parameters appropriate for $YBa_2Cu_3O_7$ ($\lambda = 1500$Å, $\xi = 16$Å) are shown in Fig. 3. While at low fields G depends smoothly on β with the expected minimum at $\beta = 60°$, the dependence of G on β, and similarly the dependence of the equilibrium β on H, are no longer smooth in fields of several tesla. Rather, these functions become extremely sensitive to the core cutoff. In the field range covered in our experiments, the London approximation is thus no longer applicable, and the equilibrium structure of the vortex lattice becomes very sensitive to the spatial variation of the superconducting order parameter near the vortex core.

The shape of the vortex core in turn depends on the microscopic electronic structure of the superconductor, that is, the shape of the Fermi surface and the energy gap. $NbSe_2$, for example, has a very complicated sixfold symmetric Fermi surface, and scanning tunneling microscopy measurements have directly revealed hexagonal vortex cores [19]. In this material the vortex lattice thus retains the sixfold symmetric triangular structure predicted by the London model even as vortex core effects become relevant in high magnetic fields. By contrast, the vortex core in $YBa_2Cu_3O_7$ must reflect the fourfold symmetry of the crystal lattice, so that the vortex lattice symmetry must change in sufficiently high magnetic fields.

A quantitative understanding of the vortex lattice structure can be obtained only by solving the gap equation at the appropriate temperature and magnetic field, which is, in general, very difficult. Fortunately, a large body of work on anisotropy effects in superconductors already exists [2–4]. Whereas a uniaxial anisotropy can be treated within the London (or Ginzburg-Landau) theory, a treatment of the cubic anisotropies often observed in low-κ superconductors (and, by analogy, the square in-plane anisotropy in $YBa_2Cu_3O_7$) requires nonlocal corrections to the Ginzburg-Landau equations. Two such theories have been proposed: While Takanaka [3] considers the effects of Fermi surface anisotropy only, Teichler [4] also takes an anisotropic phonon spectrum and an anisotropic

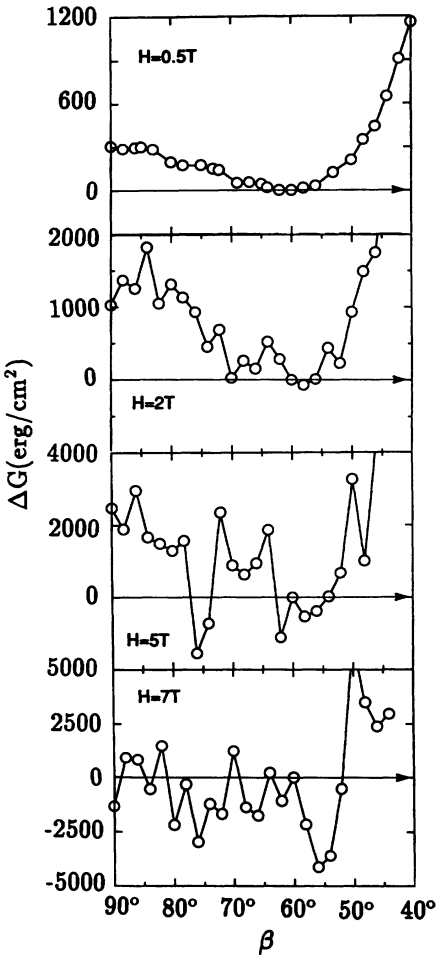

FIG. 3. Numerically computed Gibbs free energy densities of vortex lattices with centered rectangular symmetry, as a function of the angle β between primitive vectors (Fig. 2), relative to the triangular lattice ($\beta = 60°$). The calculations are based on the London model with $\lambda = 1500$ Å and $\xi = 16$ Å. The numerical errors are much smaller than the symbol size.

electron-phonon interaction into account when solving the gap equation in a magnetic field. In qualitative agreement with our data as well as observations in low-κ superconductors [6], both theories predict that structures with centered rectangular symmetry have a lower free energy than triangular and square lattices as the field is oriented in a fourfold crystalline direction. (Oblique lattice structures have thus far not been considered.) A simple analysis [15] reveals that the Fermi surface anisotropy extracted from photoemission experiments [20] is too small to quantitatively explain our data. An in-plane anisotropy of the penetration depth may contribute to the quantitative discrepancy between Takanaka's theory and our observations: A variety of measurements has revealed ratios ranging from ~1.1 [7] to ~1.5 [21] for the penetration depths in the (100) and (010) crystallographic directions. While this anisotropy has to be taken into account in a complete analysis, the structure observed in our experiments is certainly different from the one expected on the basis of an in-plane penetration depth anisotropy alone [13].

Teichler [4] shows that, at least for low-κ superconductors, the orientation dependent part of the intervortex interaction follows the coherence length anisotropy, which in turn can be separated into terms originating from the Fermi surface anisotropy and terms originating from the anisotropy of the energy gap. In view of the large gap anisotropy, observed in cuprate materials such as $Bi_2Sr_2CaCu_2O_{8+\delta}$ [22] gap-dependent effects are expected to dominate in $YBa_2Cu_3O_7$, and the nearest-neighbor direction of the vortex lattice is expected to be the crystalline (110) direction, i.e., the direction of minimum energy gap [22] and maximum coherence length. Although this analysis will likely need substantial modifications in the case of $YBa_2Cu_3O_7$ (especially if the minimum gap is zero), it provides a natural explanation of the observed orientation of the vortex lattice.

There is, therefore, no need to invoke twin boundaries as the origin of the coupling between vortex lattice and crystal lattice orientations, as suggested previously [9–11] on the basis of incomplete data. The twin boundary picture is difficult to reconcile with our observation [10] that the vortex lattice remains coupled to the crystal lattice even as the magnetic field is tilted by up to 40° with respect to the twin boundaries, where no influence of twin boundaries on the morphology of the vortex lattice is discernible. Further, our present observation that the vortex lattice structure is field independent as the intervortex distance varies from comparable to the average twin boundary spacing (~900 Å [10]) at 0.5 T to substantially smaller than the twin boundary spacing at 5 T argues against an essential influence of twin boundaries on the vortex lattice structure. We also note that Bitter decoration patterns of twin-free regions of $YBa_2Cu_3O_7$ in the highest magnetic fields accessible to this technique (~0.0065 T) reveal patterns surprisingly similar to the ones we observe: The data of Dolan *et al.* [7] are, in fact, completely consistent with the structure of Fig. 2 with $\beta = 65° \pm 5°$. This suggests that our analysis remains valid down to very low fields, consistent with a large gap anisotropy.

In conclusion, the combination of experimental and numerical data strongly suggests that spatial variations of the superconducting order parameter near the vortex core significantly influence both the structure and the orientation of the vortex lattice in $YBa_2Cu_3O_7$ in magnetic fields of the order of 1 T.

We are grateful to C. Glinka and J. Rush for their support and advice and to V. J. Emery, H. F. Hess, D. E. Moncton, N. P. Ong, and M. Yethiraj for helpful discussions. The work at Princeton was supported by the Advanced Research Projects Agency and the Air Force Office of Scientific Research under Grants AFOSR No. F49620-90-C-0079 and No. F49620-93-I-0259. This work is based upon activities supported by the National Science Foundation under Agreement No. DMR-9122444.

[1] W. H. Kleiner, L. M. Roth, and S. H. Autler, Phys. Rev. **133**, A1226 (1964).
[2] *Anisotropy Effects in Superconductors*, edited by H. W. Weber (Plenum, New York, 1977).
[3] K. Takanaka, Prog. Theor. Phys. **46**, 1301 (1971); **49**, 64 (1973); **50**, 365 (1973).
[4] H. Teichler, Philos. Mag. **30**, 1209 (1974); **31**, 775 (1975); **31**, 789 (1975); K. Fischer and H. Teichler, Phys. Lett. **58A**, 402 (1976); see also T. Koyama *et al.*, Phys. Rev. B **20**, 918 (1979).
[5] B. Obst, Phys. Status Solidi B **45**, 467 (1971).
[6] J. Schelten, G. Lippmann, and H. Ullmaier, J. Low Temp. Phys. **14**, 213 (1974).
[7] G. J. Dolan *et al.*, Phys. Rev. Lett. **62**, 2184 (1989).
[8] C. A. Bolle *et al.*, Phys. Rev. Lett. **71**, 4039 (1993).
[9] E. M. Forgan *et al.*, Physica (Amsterdam) **185–189C**, 247 (1991); M. Yethiraj *et al.*, Phys. Rev. Lett. **70**, 857 (1993).
[10] B. Keimer *et al.*, Science **262**, 83 (1993).
[11] M. Yethiraj *et al.*, Phys. Rev. Lett. **71**, 3019 (1993).
[12] H. F. Hess, C. A. Murray, and J. V. Waszczak, Phys. Rev. Lett. **69**, 2138 (1992); P. L. Gammel *et al.*, *ibid.* **72**, 278 (1994).
[13] L. J. Campbell, M. M. Doria, and V. G. Kogan, Phys. Rev. B **38**, 2439 (1988).
[14] J. S. Pedersen, D. Posselt, and K. Mortensen, J. Appl. Crystallogr. **23**, 321 (1990).
[15] B. Keimer *et al.*, J. Appl. Phys. **76**, 6778 (1994).
[16] J. Matricon, Phys. Lett. **9**, 289 (1964).
[17] E. H. Brandt, Phys. Status Solidi B **51**, 345 (1972).
[18] M. Tinkham, *Introduction to Superconductivity* (Krieger, Malabar, 1975).
[19] H. F. Hess, R. B. Robinson, and J. V. Waszczak, Phys. Rev. Lett. **64**, 2711 (1990).
[20] J. C. Campuzano *et al.*, Phys. Rev. Lett. **64**, 2308 (1990).
[21] K. Zhang *et al.*, Phys. Rev. Lett. **73**, 2484 (1994).
[22] Z.-X. Shen *et al.*, Phys. Rev. Lett. **70**, 1553 (1993).

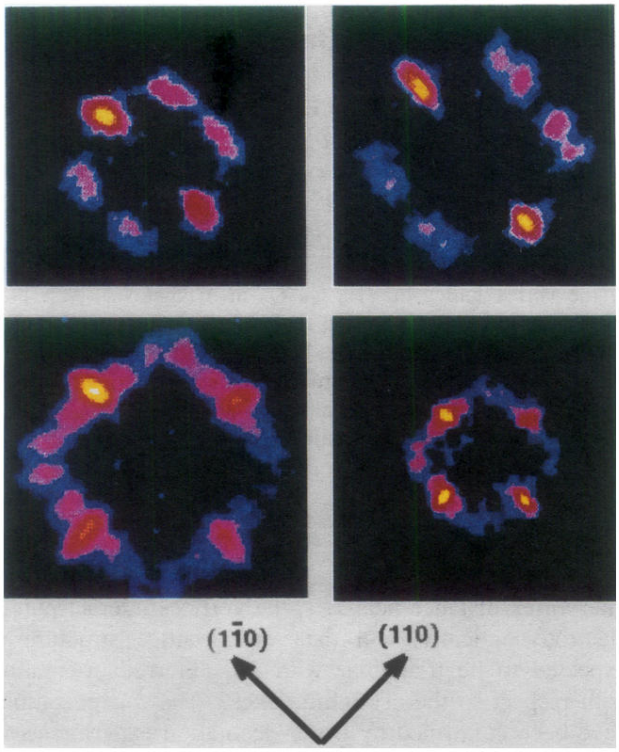

FIG. 1. SANS diffraction patterns of the vortex lattice taken for $H = 0.5$ T (top left), $H = 2$ T (top right and bottom left), and $H = 4.3$ T (bottom right), under experimental conditions described in the text. The temperature is 4.2 K, and the magnetic field is perpendicular to the page. Patterns in the bottom row are taken with the magnetic field parallel to the c axis, while for the patterns in the top row the c axis subtends angles of $\sim 10°$ (left) [10] or 20° (right) with the field. The (110) and (1$\bar{1}$0) directions of the crystal lattice are indicated. The Bragg angles corresponding to the diffraction spot positions depend on the experimental conditions, so that they cannot be directly inferred from the patterns shown or compared between panels. For clarity the data were digitally smoothed on a scale comparable to the geometrical resolution.